Science Advances
AAAS

advances.sciencemag.org/cgi/content/full/7/3/eabc8590/DC1

Supplementary Materials for

Overlap of NatA and IAP substrates implicates N-terminal acetylation in protein stabilization

Franziska Mueller, Alexandra Friese, Claudio Pathe, Richard Cardoso da Silva, Kenny Bravo Rodriguez, Andrea Musacchio*, Tanja Bange*

*Corresponding author. Email: andrea.musacchio@mpi-dortmund.mpg.de (A.M.); tanja.bange@med.uni-muenchen.de (T.B.)

Published 15 January 2021, *Sci. Adv.* **7**, eabc8590 (2021)
DOI: 10.1126/sciadv.abc8590

The PDF file includes:

Other Supplementary Material for this manuscript includes the following:

(available at advances.sciencemag.org/cgi/content/full/7/3/eabc8590/DC1)

Supplementary Discussion

In their impressive recent analysis, Timms and co-workers (*61*) used the high-throughput Global Protein Stability (GPS) methodology (*73*) to characterize degron motifs in human proteins. The GPS system adopts the ubiquitin (Ub) fusion technique (*74*) ("Ub-GPS"), whereby proteolytic cleavage of the N-terminal Ub by endogenous deubiquitinating enzymes leads to exposure of peptides at the N-terminus of GFP, whose levels are subsequently measured against an internal reference.

This powerful approach allowed the authors to compare the relative stability of GFP fusion proteins in which any N-terminal residue (X) was or was not preceded by Met after removal of Ub (*74*). Their results provide unequivocal evidence that when X is one of the following residues, C, V, G, P, T, A, S, or M (a class herewith referred to arbitrarily as Z and coinciding with substrates of methionine aminopeptidase), no large differences in the stability of the MX and X pairs is observed, and, importantly, that both are among the most stable fusions (*61*).

This observation may seem to contradict our conclusion that sequences starting with several of the residues in this class (most notably, but not limitedly to, A and S) have the potential to be destabilizing if not acetylated. Indeed, post-translational proteolytic removal of the fused Ub ought to generate the perfect IBM-like motifs for IAPs, and if these were destabilizing, strong differences in the stability of MX and X sequences would be expected.

While this concern requires further investigations, we reason that in the absence of evidence on when precisely the Ub moiety is removed from the Ub-GPS fusion proteins, whether the resulting N-termini will be treated "post-translationally" or "co-translationally" is unknown. Because Ub (iso)peptidases are known to be very active enzymes, and Ub is only ~70 residues, it is plausible that the endoproteolytic separation of Ub from the rest of the protein occurs while the protein is being translated. In this case, the resulting N-termini will be treated as if they had been the "real" N-termini on the nascent chain, including cleavage of Met^i for the MZ sequences, and acetylation for both the "natural" Z sequences or for those generated after removal of Met^i. This would provide a simple explanation for why MZ and Z sequences have comparable stability and why they do not activate IAPs.

This interpretation would also fit the other crucial observation in the analysis by Timms and co-workers that when N-terminal myristylation of glycine is inhibited, the unmodified glycine acts as a potent degron, regardless of whether it is preceded by methionine in the Ub-GPS system (*61*), at least implying that Met is removed. The authors additionally identified $CUL2^{ZYG11B}$ and $CUL2^{ZER1}$ as Ub-ligases that target unmodified N-terminal glycine, and demonstrated that their depletion leads to complete or near-complete stabilization of peptide-GFP fusion constructs. However, combined mutations of ZYG11B and ZER1 only resulted in partial re-stabilization of endogenous proteins with N-terminal glycine when N-terminal myristylation of glycine was inhibited. In our analysis of BIR-domain binding partners in NatA-depleted cells, we also identify several proteins predicted to have N-terminal glycine (Supplementary Table 5), including proteins predicted to be myristoylated. This suggests the interesting possibility that IAPs complement $CUL2^{ZYG11B}$ and $CUL2^{ZER1}$ as Ub-ligases in the degradation of glycine N-degrons.

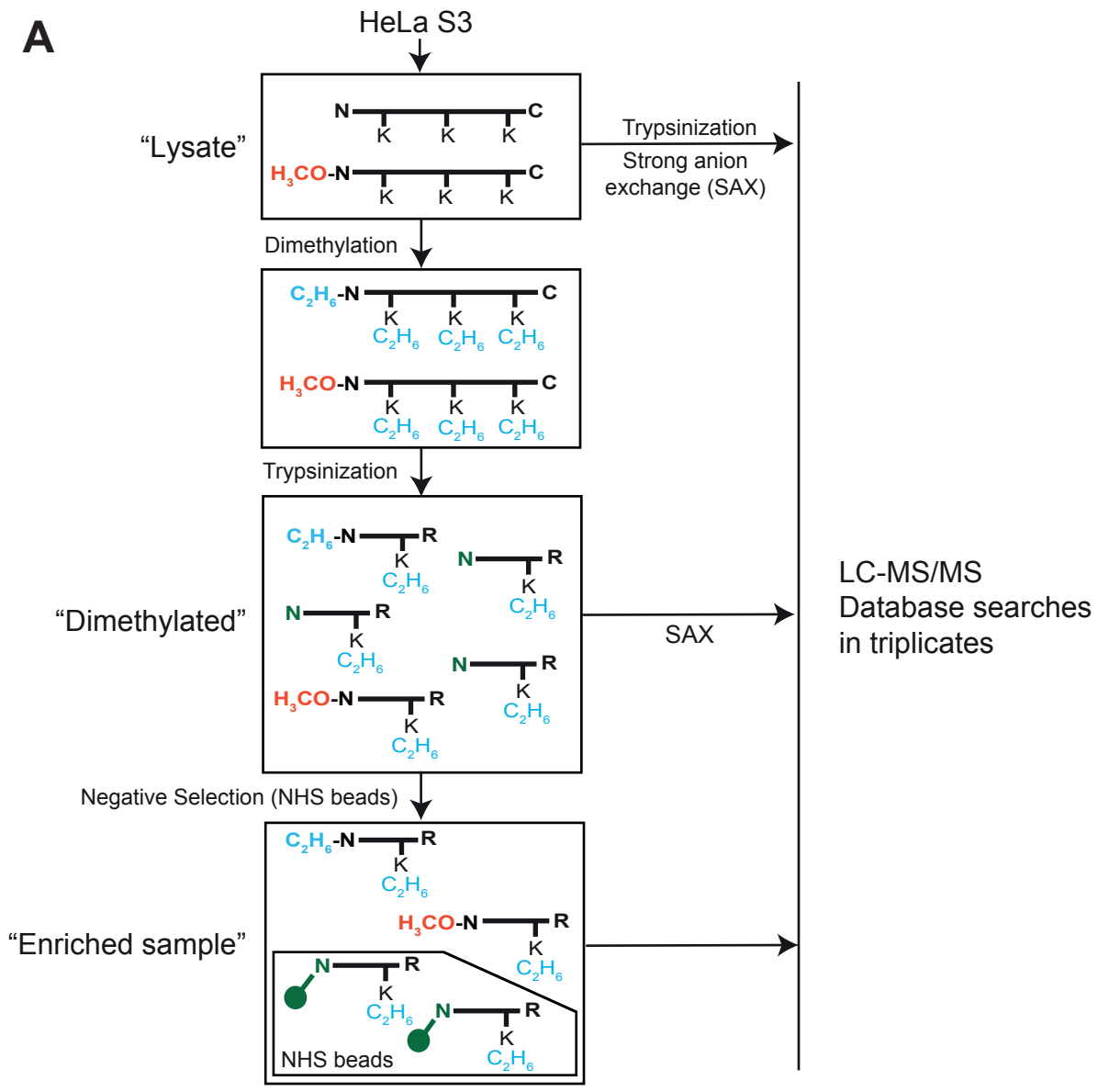

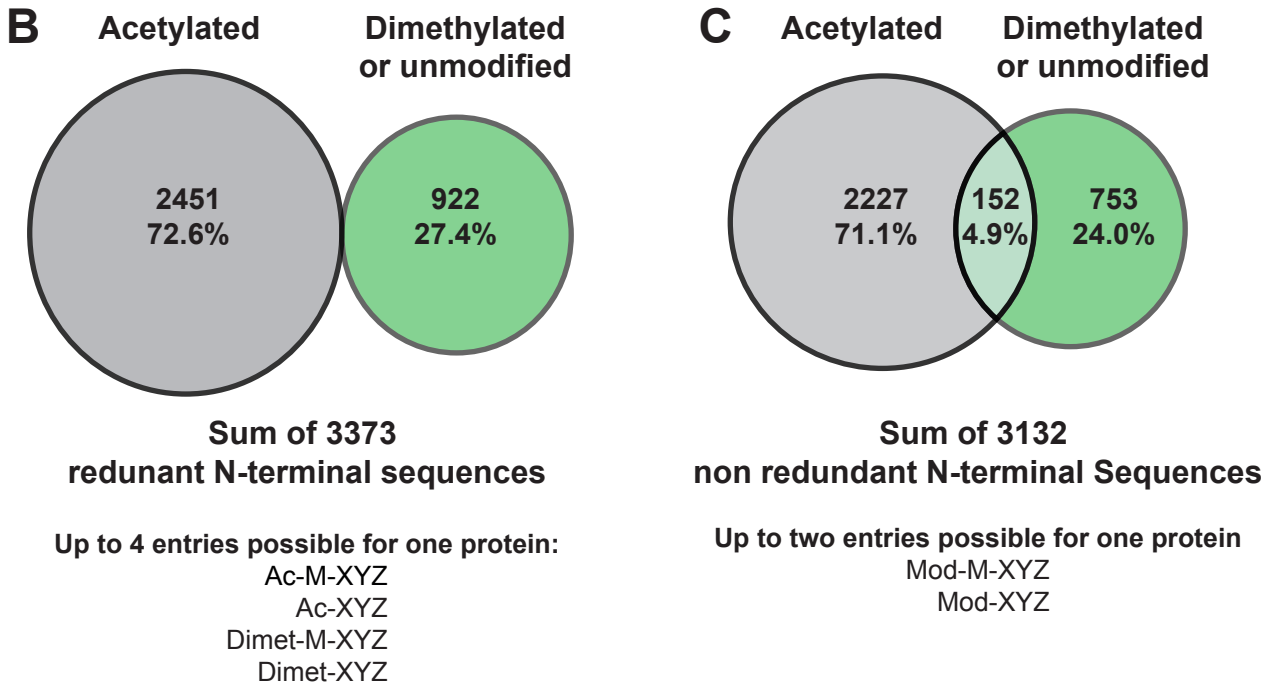

Sum of 3373 redunant N-terminal sequences

Up to 4 entries possible for one protein:
Ac-M-XYZ
Ac-XYZ
Dimet-M-XYZ
Dimet-XYZ

Sum of 3132 non redundant N-terminal Sequences

Up to two entries possible for one protein
Mod-M-XYZ
Mod-XYZ

Mueller et al.
Figure S1

Supplementary Figure Legends

Figure S1

Experimental scheme and numbers of the HeLa N-terminome measured by MS

(A) Scheme of experimental design for HeLa N-terminome measurements by MS (SAX: strong anion exchange). **(B)** Venn diagram with numbers of identified peptides and percentages of acetylated and unmodified (di-methylated or mono-methylated) peptides is presented. Every protein can have up to four entries: N-terminus with or without methionine and dimetylated or acetylated. **(C)** Venn diagram with numbers of identified peptides and percentages of acetylated, unmodified (di-methylated or mono-methylated) and the overlap of peptides identified with both modifications is shown. Entries from (**B**) have been collapsed to unique sequences starting with methionine or with the second amino acid. Data have been further collapsed to a non-redundant protein list shown in Figure 1A**.**

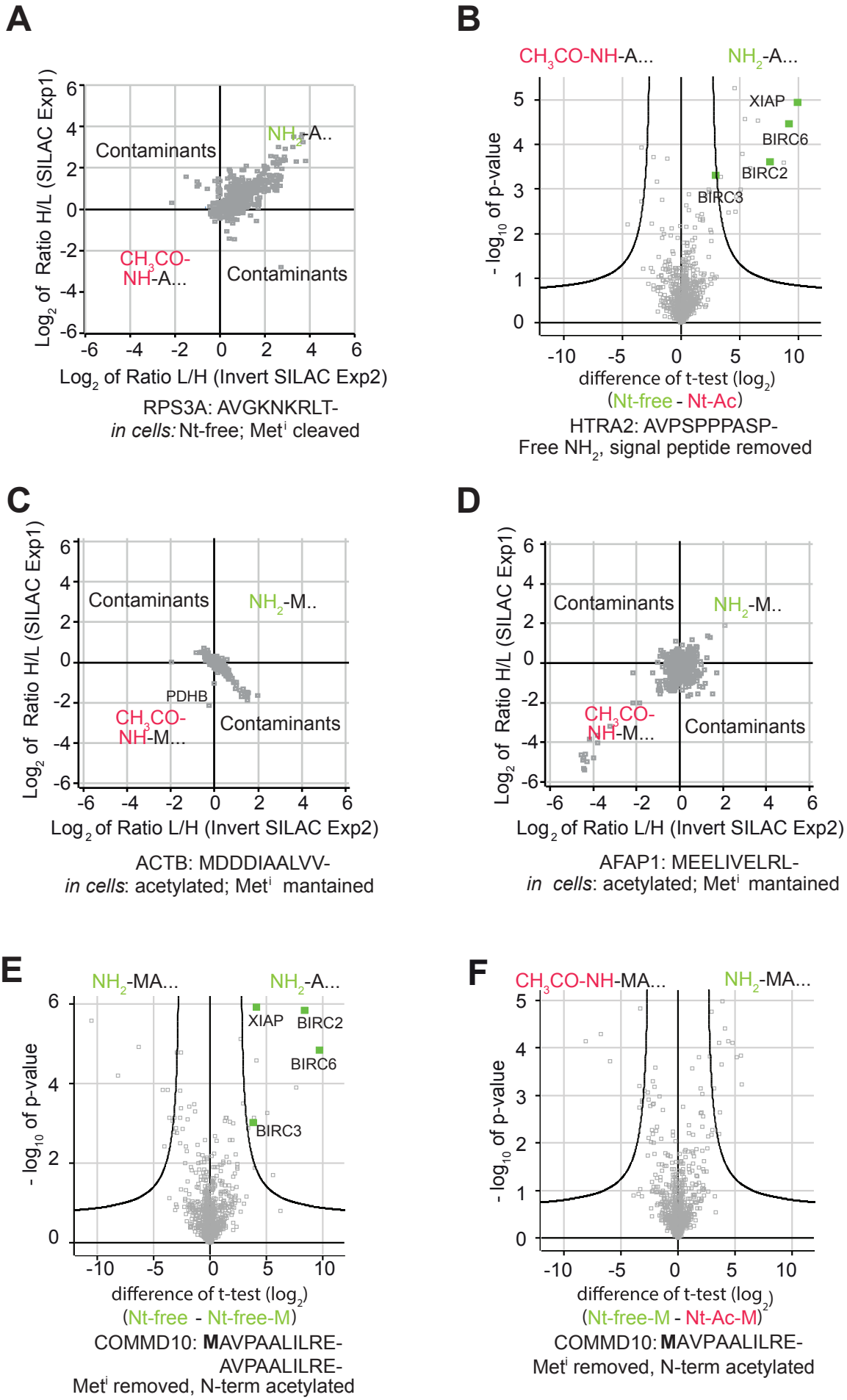

Mueller et al.
Figure S2

Figure S2

Control peptide pull-downs of Nt-free and Nt-Ac peptides

(A-D) Peptide pull-downs with Nt-free (Nt-free refers here and elsewhere to a free Nt-α-amino group at the N-terminus of a peptide/protein) and Nt-Ac peptides from RPS3A (**A**), HTRA2 (**B**), ACTB (**C**), AFAP1 (**D**). (**A**), (**C**) and (**D**) are SILAC experiments and two experiments with inverted labelling were plotted against each other. Experiments were repeated twice. (**B**) is a volcano plot of label-free triplicates. **(E)** Volcano plots with pull-downs from Nt-free COMMD10 ("wt" N-terminus) and Met^i retaining COMMD10 are shown. **(F)** Pull-downs of Nt-free and Nt-Ac Met^i retaining COMMD10 are shown. T-test cut-off for all volcano plots was FDR < 0.01, S0 > 2). IAPs are highlighted in green. All experiments were performed at least in triplicates. All quantified proteins and binders of the pull-downs are listed in Supplementary Table 2.

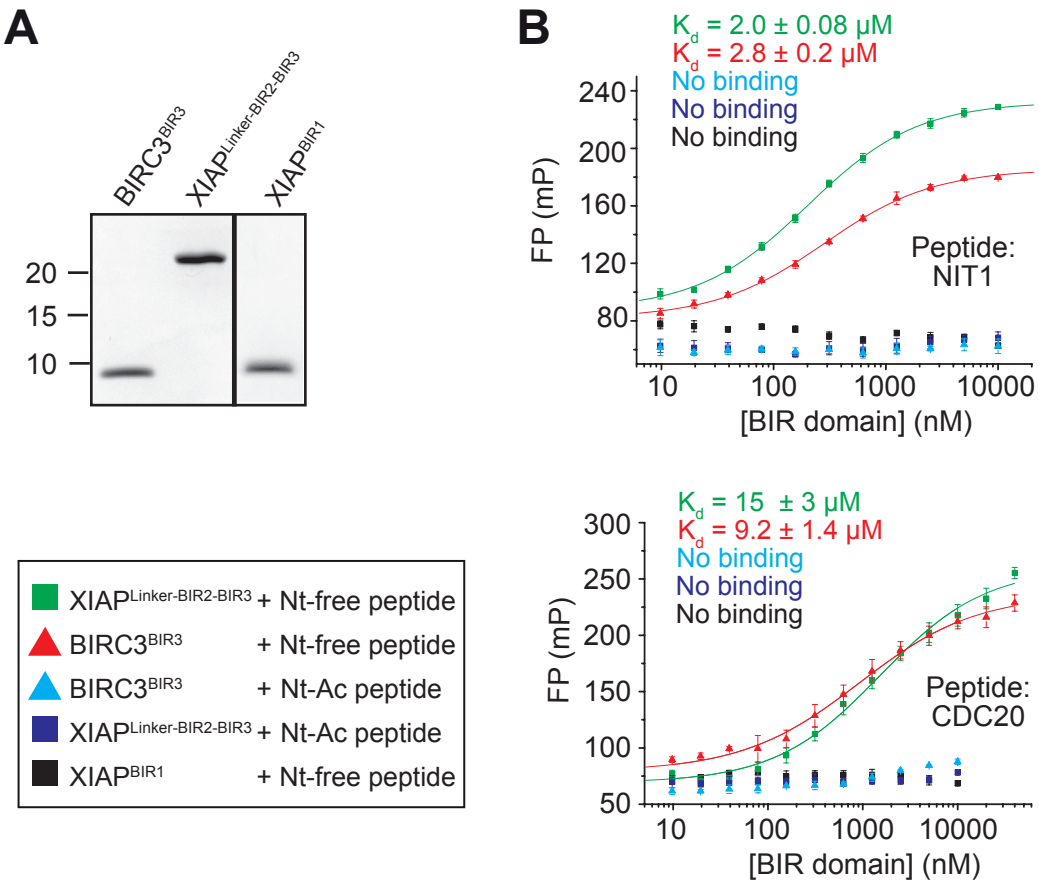

Mueller et al.
Figure S3

Figure S3

Nt-free N-terminal peptides bind to BIR domains *in vitro*

(A) Coomassie-stained gel of purified BIR domain constructs. **(B)** 20 nM of FITC-labelled peptides (Nt-Ac or Nt-free) of NIT1 (upper panel) or CDC20 (lower panel) were incubated for 30 min with increasing amounts of His-tag BIR domain constructs ($XIAP^{Linker\text{-}BIR2\text{-}BIR3}$, $BIRC^{BIR3}$, $XIAP^{BIR1}$). Fluorescence polarization was measured at excitation and emission wavelength of 470 and 525 nm, respectively, and data (millipolarization units, mP) were plotted as function of BIR domain concentration and fitted with a logistic fit with Origin7.0. K_d values are reported in the figures and summarized in Supplementary Table 3. Panel lower left side: legend of used constructs and combinations for (**B**).

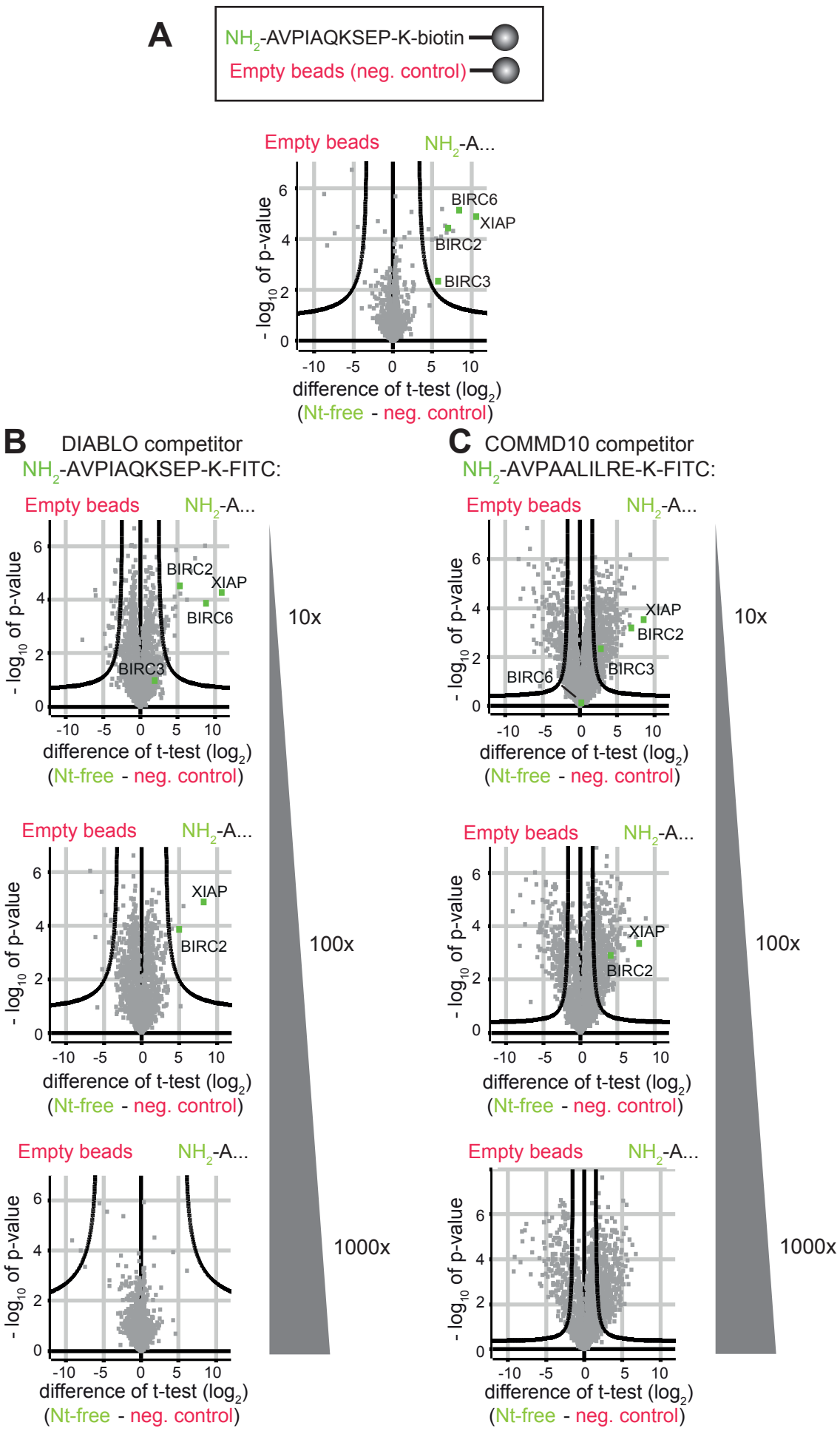

Mueller et al.
Figure S4

Figure S4

The Nt-free N-terminus of COMMD10 competes with DIABLO for IAP binding

(A) Volcano plot of peptide pull-downs using Nt-free biotinylated DIABLO versus beads as control. **(B,C)** Lysates have been incubated before pull-down with 10-fold, 100-fold and 1000-fold molar excess of DIABLO-FITC as control (**B**) or COMMD10-FITC (**C**). Volcano plots (cut-off: FDR < 0.01, S0 > 2) are shown for every pull-down. IAPs are highlighted in green. All experiments were performed at least in triplicates. All quantified proteins and binders are listed in Supplementary Table 4.

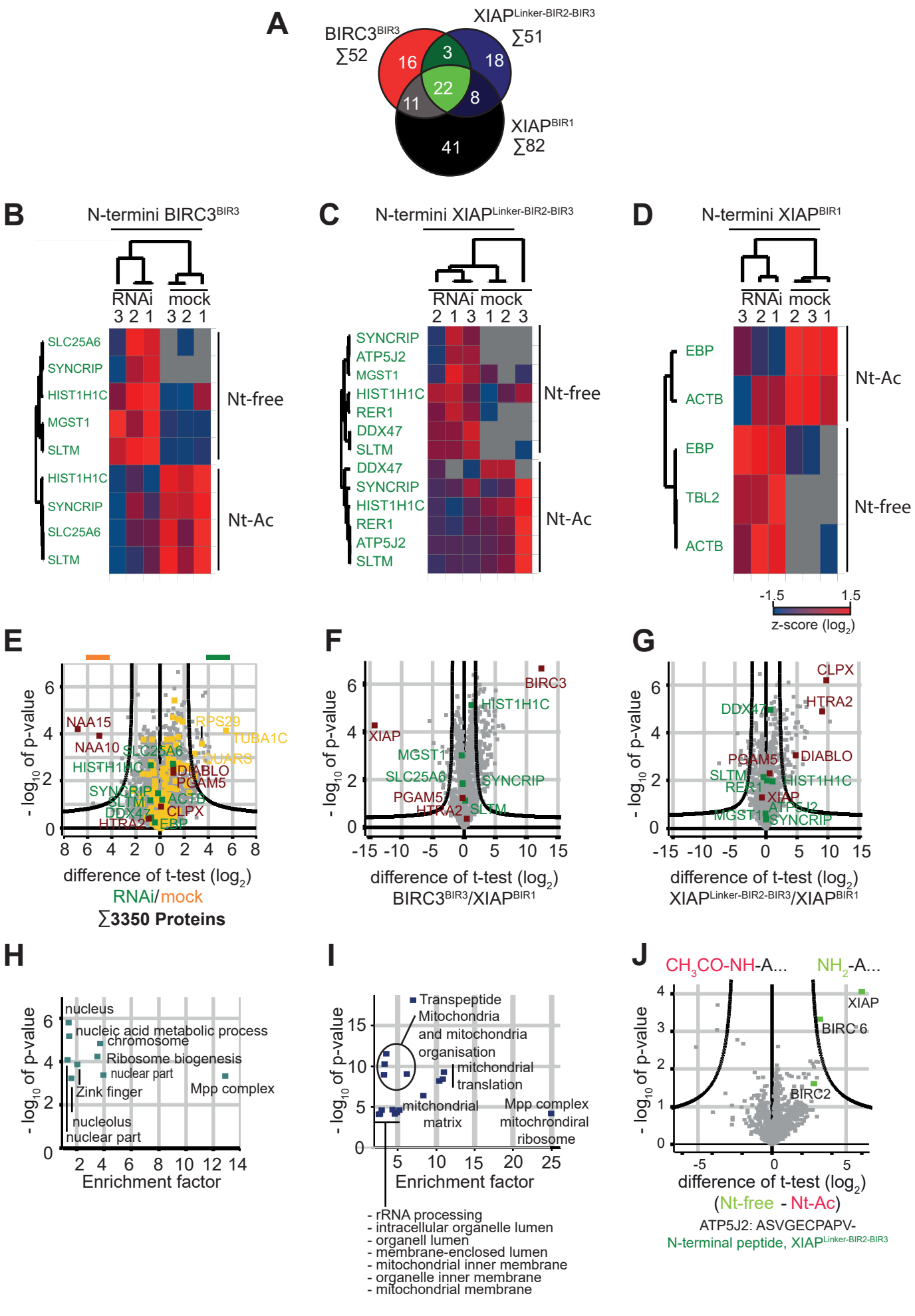

Mueller et al.
Figure S5

Figure S5

Additional information to His-tag BIR domain pull-downs and whole proteome analysis of NatA RNAi and mock cells

(A) A Venn diagram summarizing number of significant protein binders from the samples treated with RNAi for NatA versus mock from $BIRC3^{BIR3}$, $XIAP^{Linker\text{-}BIR2\text{-}BIR3}$ and $XIAP^{BIR1}$ (t-test cut-off: FDR < 0.05, S0 > 2) marked in yellow in Figure 3 and reported in Supplementary Table 5 is shown. **(B, C, D)** Unsupervised hierarchical clustering of intensities (raw intensities in log_2 and z-scored without imputation) from Nt-free and Nt-Ac N-terminal peptides identified as significant binders to the BIR domains in their unmodified form (Figure 3B-D and 3F-H). **(E)** Whole proteome analysis of RNAi and mock treated HeLa lysates (t-test cut-off: FDR < 0.05, S0 > 2). All identifications are reported in Supplementary Table 6. **(F,G)** Volcano plots (t-test cut-off: FDR < 0.05, S0 > 2) from pull-downs using HeLa cell lysates comparing binding of proteins to $BIRC3^{BIR3}$ and $XIAP^{BIR1}$ (**F**) or $XIAP^{Linker\text{-}BIR2\text{-}BIR3}$ and $XIAP^{BIR1}$ (**G**). Color codes are the same as in Figure 3. Dark red: baits and known interactors, green: significant peptides comparing RNAi versus mock for $BIRC3^{BIR3}$ or $XIAP^{Linker\text{-}BIR2\text{-}BIR3}$ (Figure 3B-C), respectively. Yellow: significant binding proteins comparing RNAi versus mock for $BIRC3^{BIR3}$ or $XIAP^{Linker\text{-}BIR2\text{-}BIR3}$ (Figure 3F-G), respectively. **(H,I)** Enrichment analysis for significant binders to $BIRC3^{BIR3}$ versus the whole data set comparing to $XIAP^{BIR1}$ (Fisher Exact test**,** Benjamini-Hochberg FDR < 0.02) (**H**) and significant binders to $XIAP^{Linker\text{-}BIR2\text{-}BIR3}$ versus the whole data set comparing to $XIAP^{BIR1}$ (Fisher Exact test**,** Benjamini-Hochberg FDR < 0.01) (**I**). The most enriched terms from Keywords, GOCC (cellular compartment) and GOMF (molecular function) are shown. A complete list of identified proteins and the enrichment analysis can be found in Supplementary Table 6. **(J)** Volcano plot of peptide pull-down with free Nt-α-amino (Nt-free) and Nt-ac peptides from ATP5J2. T-test cut-off values: FDR < 0,05, S0 > 2. IAPs are highlighted in green (additional pull-down to Figure 4 and reported with all identifications in Supplementary Table 7).

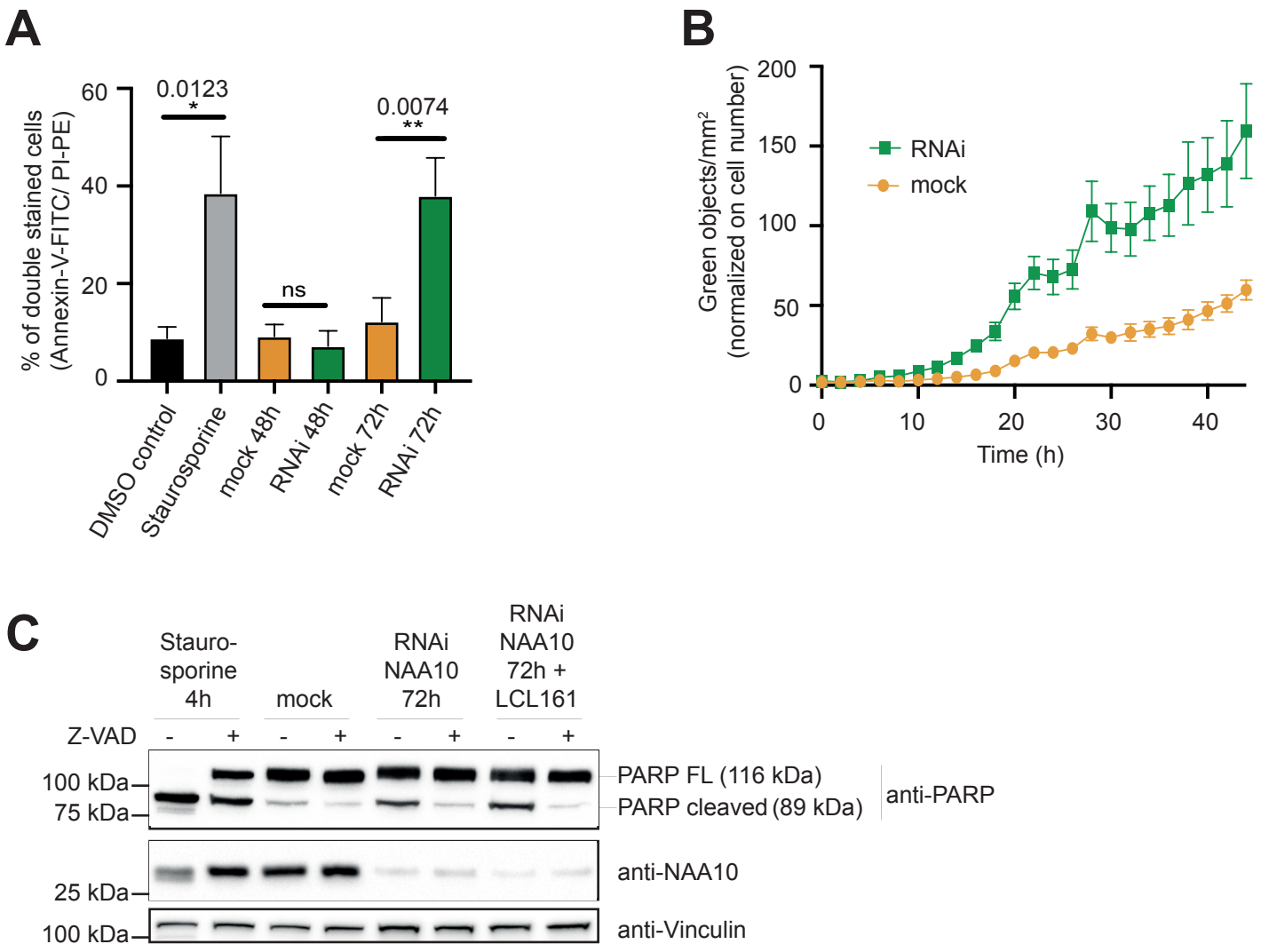

Mueller et al.
Figure S6

Figure S6

RNAi of NatA induces apoptosis

(A) Column diagram of three independent flow cytometry analysis of HeLa cells transfected with RNAi for NatA (25 nM) or mock. Cells were treated for the indicated times. As control, cells were treated with 300 nM Staurosporine for 4 hours. Cells were stained with Annexin-V-FITC and Propidium Iodid and analyzed by flow cytometry. An unpaired t-test was used to determine significant apoptosis. Ns: not significant, *: p-value < 0.05, **: p-value < 0.01. **(B)** HeLa cells treated with RNAi for NatA or mock were analyzed in an IncuCyte® reader. Apoptosis was monitored by a fluorescent Casp3/7 reagent every two hours over 48 hours. Numbers were normalized to cell count by using a nuclear stain in parallel. Results of three independent experiments each in triplicate are shown. **(C)** HeLa cells have been treated for 72 hours with NAA10 RNAi, mock or 4 hours Staurosporine as control or with a combination of 72 hours NAA10 RNAi and 24 hours LCL161. In addition, all conditions have been as well treated or not with the pan-caspase inhibitor Z-VAD. IB anti-PARP, anti-NAA10 and anti-Vinculin are shown.

Supplementary Tables

Supplementary Table 1

N-terminal proteome analysis

List of all MS identified N-termini with their N-terminal modifications considering proteins starting with position 1 and 2. Used proteins/peptides in the paper are highlighted in green.

Supplementary Table 2

Pull-downs with Nt-free and Nt-Ac peptides using HeLa lysates

All identified and quantified proteins for the indicated pull-downs from Figure 1D-I and Figure S2A-F are listed. Color codes are corresponding to the figures.

Supplementary Table 3

Summary of fluorescence polarization assay

Summary of all measured K_d values.

Supplementary Table 4

Competition assay

All identified and quantified proteins for the indicated competition pull-downs from Figure S4 are shown. Color codes are corresponding to Figure S4.

Supplementary Table 5

Pull-down with His-tag BIR-domains using RNAi or mock treated cellular lysates

All identified and quantified N-terminal peptides and proteins for the indicated pull-downs from Figure 3B-D and 3F-H are shown. Color codes are corresponding to the figures.

Supplementary Table 6

Pull-down experiments using $XIAP^{Linker\text{-}BIR2\text{-}BIR3}$, $XIAP^{BIR1}$ and $BIRC3^{BIR3}$ with enrichment analysis and full proteome analysis of RNAi and mock treated lysates

All identified and quantified proteins for the pull-downs and whole proteome analysis and enrichment analysis for the pull-downs from Figure S5 are reported.

Supplementary Table 7

Pull-downs with Nt-free and Nt-Ac peptides using HeLa lysates

All identified and quantified proteins for the pull-downs from Figure 4 and Figure S5J are shown.

Glossary of Excel columns

Protein Names: Name(s) of protein(s) contained within the group.

Gene Name: Name of gene(s) this peptide(s) is associated with.

Majority protein IDs: These are the UNIPROT ID(s) of those proteins that have at least half of the peptides that the leading protein has.

significant in t-test: +, proteins which are significant in a t-test with certain cut-off values, stated in the figures and the column header.

$-\log_{10}$ of t-test p-value: inverted**,** logarithmized p-values of the t-test between two conditions plotted in the volcano plots in the figures on the y-axis.

Student's t-test difference: $\log_2$ of the difference between the two conditions plotted on the x-axis in the volcano plots.

Peptides: Total number of peptide sequences associated with the protein group.

Sequence coverage (%): Percentage of the sequence that is covered by the identified peptides of the best protein sequence contained in the group.

Mol. weight (kDa): Molecular weight of the leading protein sequence contained in the protein group.

MS/MS count: Number of MS/MS events for the protein group or peptide.

Sequence: Identified aa of the peptide.

Modifications: Post-translational modifications contained within the sequence. When no modifications exist, this is set to “unmodified”.

Mass: Charge corrected mass of the precursor ion.

PEP: Posterior Error Probability of the identification. This value essentially operates as a p-value, where smaller is more significant.

Score: Andromeda score for the best identified among the associated MS/MS spectra.

LFQ intensities (*70*): Summed up extracted Ion Current (XIC) of all isotopic clusters associated with the identified AA sequence and validated for relative quantification of proteins, peptides are reported with intensities no LFQ values can be determined.

REFERENCES AND NOTES

1. Q. Xiao, F. Zhang, B. A. Nacev, J. O. Liu, D. Pei, Protein N-terminal processing: Substrate specificity of *Escherichia coli* and human methionine aminopeptidases. *Biochemistry* **49**, 5588–5599 (2010).

2. H. Aksnes, R. Ree, T. Arnesen, Co-translational, post-translational, and non-catalytic roles of N-terminal acetyltransferases. *Mol. Cell* **73**, 1097–1114 (2019).

3. S. Varland, H. Aksnes, F. Kryuchkov, F. Impens, D. Van Haver, V. Jonckheere, M. Ziegler, K. Gevaert, P. Van Damme, T. Arnesen, N-terminal acetylation levels are maintained during acetyl-CoA deficiency in *Saccharomyces cerevisiae*. *Mol. Cell. Proteomics* **17**, 2309–2323 (2018).

4. C. H. Yi, H. Pan, J. Seebacher, I.-H. Jang, S. G. Hyberts, G. J. Heffron, M. G. V. Heiden, R. Yang, F. Li, J. W. Locasale, H. Sharfi, B. Zhai, R. Rodriguez-Mias, H. Luithardt, L. C. Cantley, G. Q. Daley, J. M. Asara, S. P. Gygi, G. Wagner, C.-F. Liu, J. Yuan, Metabolic regulation of protein N-alpha-acetylation by Bcl-xL promotes cell survival. *Cell* **146**, 607–620 (2011).

5. A. Hershko, H. Heller, E. Eytan, G. Kaklij, I. A. Rose, Role of the alpha-amino group of protein in ubiquitin-mediated protein breakdown. *Proc. Natl. Acad. Sci. U.S.A.* **81**, 7021–7025 (1984).

6. L. M. Myklebust, P. Van Damme, S. I. Støve, M. J. Dörfel, A. Abboud, T. V. Kalvik, C. Grauffel, V. Jonckheere, Y. Wu, J. Swensen, H. Kaasa, G. Liszczak, R. Marmorstein, N. Reuter, G. J. Lyon, K. Gevaert, T. Arnesen, Biochemical and cellular analysis of Ogden syndrome reveals downstream Nt-acetylation defects. *Hum. Mol. Genet.* **24**, 1956–1976 (2015).

7. S. Goetze, E. Qeli, C. Mosimann, A. Staes, B. Gerrits, B. Roschitzki, S. Mohanty, E. M. Niederer, E. Laczko, E. Timmerman, V. Lange, E. Hafen, R. Aebersold, J. Vandekerckhove, K. Basler, C. H. Ahrens, K. Gevaert, E. Brunner, Identification and functional characterization of N-terminally acetylated proteins in *Drosophila melanogaster*. *PLOS Biol.* **7**, e1000236 (2009).

8. A. Shemorry, C.-S. Hwang, A. Varshavsky, Control of protein quality and stoichiometries by N-terminal acetylation and the N-end rule pathway. *Mol. Cell* **50**, 540–551 (2013).

9. C.-S. Hwang, A. Shemorry, A. Varshavsky, N-terminal acetylation of cellular proteins creates specific degradation signals. *Science* **327**, 973–977 (2010).

10. I. Kats, A. Khmelinskii, M. Kschonsak, F. Huber, R. A. Knieß, A. Bartosik, M. Knop, Mapping degradation signals and pathways in a Eukaryotic N-terminome. *Mol. Cell* **70**, 488–501.e5 (2018).

11. N. Mischerikow, A. J. Heck, Targeted large-scale analysis of protein acetylation. *Proteomics* **11**, 571–589 (2011).

12. P. Van Damme, T. Arnesen, K. Gevaert, Protein alpha-N-acetylation studied by N-terminomics. *FEBS J.* **278**, 3822–3834 (2011).

13. P. Van Damme, M. Lasa, B. Polevoda, C. Gazquez, A. Elosegui-Artola, D. S. Kim, E. De Juan-Pardo, K. Demeyer, K. Hole, E. Larrea, E. Timmerman, J. Prieto, T. Arnesen, F. Sherman, K. Gevaert, R. Aldabe, N-terminal acetylome analyses and functional insights of the N-terminal acetyltransferase NatB. *Proc. Natl. Acad. Sci. U.S.A.* **109**, 12449–12454 (2012).

14. P. F. Lange, P. F. Huesgen, C. M. Overall, TopFIND 2.0—Linking protein termini with proteolytic processing and modifications altering protein function. *Nucleic Acids Res.* **40**, D351–D361 (2012).

15. W. V. Bienvenut, D. Sumpton, A. Martinez, S. Lilla, C. Espagne, T. Meinnel, C. Giglione, Comparative large scale characterization of plant *versus* mammal proteins reveals similar and idiosyncratic *N*-α-acetylation features. *Mol. Cell. Proteomics* **11**, M111.015131 (2012).

16. A. O. Helbig, S. Rosati, P. W. W. M. Pijnappel, B. van Breukelen, M. H. T. H. Timmers, S. Mohammed, M. Slijper, A. J. R. Heck, Perturbation of the yeast N-acetyltransferase NatB induces elevation of protein phosphorylation levels. *BMC Genomics* **11**, 685 (2010).

17. T. Arnesen, P. Van Damme, B. Polevoda, K. Helsens, R. Evjenth, N. Colaert, J. E. Varhaug, J. Vandekerckhove, J. R. Lillehaug, F. Sherman, K. Gevaert, Proteomics analyses reveal the evolutionary conservation and divergence of N-terminal acetyltransferases from yeast and humans. *Proc. Natl. Acad. Sci. U.S.A.* **106**, 8157–8162 (2009).

18. The UniProt Consortium, UniProt: A worldwide hub of protein knowledge. *Nucleic Acids Res.* **47**, D506–D515 (2019).

19. H. Yamano, APC/C: Current understanding and future perspectives. *F1000Res* **8**, F1000 (2019).

20. Z. Zhang, K. Kulkarni, S. J. Hanrahan, A. J. Thompson, D. Barford, The APC/C subunit Cdc16/Cut9 is a contiguous tetratricopeptide repeat superhelix with a homo-dimer interface similar to Cdc27. *EMBO J.* **29**, 3733–3744 (2010).

21. D. C. Scott, J. T. Hammill, J. Min, D. Y. Rhee, M. Connelly, V. O. Sviderskiy, D. Bhasin, Y. Chen, S.-S. Ong, S. C. Chai, A. N. Goktug, G. Huang, J. K. Monda, J. Low, H. S. Kim, J. A. Paulo, J. R. Cannon, A. A. Shelat, T. Chen, I. R. Kelsall, A. F. Alpi, V. Pagala, X. Wang, J. Peng, B. Singh, J. W. Harper, B. A. Schulman, R. K. Guy, Blocking an N-terminal acetylation-dependent protein interaction inhibits an E3 ligase. *Nat. Chem. Biol.* **13**, 850–857 (2017).

22. D. C. Scott, J. K. Monda, E. J. Bennett, J. W. Harper, B. A. Schulman, N-terminal acetylation acts as an avidity enhancer within an interconnected multiprotein complex. *Science* **334**, 674–678 (2011).

23. J. K. Monda, D. C. Scott, D. J. Miller, J. Lydeard, D. King, J. W. Harper, E. J. Bennett, B. A. Schulman, Structural conservation of distinctive N-terminal acetylation-dependent interactions across a family of mammalian NEDD8 ligation enzymes. *Structure* **21**, 42–53 (2013).

24. J. Silke, P. Meier, Inhibitor of apoptosis (IAP) proteins-modulators of cell death and inflammation. *Cold Spring Harb. Perspect. Biol.* **5**, a008730 (2013).

25. D. Vucic, V. M. Dixit, I. E. Wertz, Ubiquitylation in apoptosis: A post-translational modification at the edge of life and death. *Nat. Rev. Mol. Cell Biol.* **12**, 439–452 (2011).

26. F. Lampert, D. Stafa, A. Goga, M. V. Soste, S. Gilberto, N. Olieric, P. Picotti, M. Stoffel, M. Peter, The multi-subunit GID/CTLH E3 ubiquitin ligase promotes cell proliferation and targets the transcription factor Hbp1 for degradation. *eLife* **7**, e35528 (2018).

27. S.-J. Chen, X. Wu, B. Wadas, J.-H. Oh, A. Varshavsky, An N-end rule pathway that recognizes proline and destroys gluconeogenic enzymes. *Science* **355**, eaal3655 (2017).

28. E. Varfolomeev, J. W. Blankenship, S. M. Wayson, A. V. Fedorova, N. Kayagaki, P. Garg, K. Zobel, J. N. Dynek, L. O. Elliott, H. J. A. Wallweber, J. A. Flygare, W. J. Fairbrother, K. Deshayes, V. M. Dixit, D. Vucic, IAP antagonists induce autoubiquitination of c-IAPs, NF-κB activation, and TNFα-dependent apoptosis. *Cell* **131**, 669–681 (2007).

29. J. E. Vince, W. W.-L. Wong, N. Khan, R. Feltham, D. Chau, A. U. Ahmed, C. A. Benetatos, S. K. Chunduru, S. M. Condon, M. M. Kinlay, R. Brink, M. Leverkus, V. Tergaonkar, P. Schneider, B. A. Callus, F. Koentgen, D. L. Vaux, J. Silke, IAP antagonists target cIAP1 to induce TNFα-dependent apoptosis. *Cell* **131**, 682–693 (2007).

30. T. Bartke, C. Pohl, G. Pyrowolakis, S. Jentsch, Dual role of BRUCE as an antiapoptotic IAP and a chimeric E2/E3 ubiquitin ligase. *Mol. Cell* **14**, 801–811 (2004).

31. J. Silke, D. L. Vaux, Two kinds of BIR-containing protein - inhibitors of apoptosis, or required for mitosis. *J. Cell Sci.* **114**, 1821–1827 (2001).

32. S. M. Srinivasula, R. Hegde, A. Saleh, P. Datta, E. Shiozaki, J. Chai, R.-A. Lee, P. D. Robbins, T. Fernandes-Alnemri, Y. Shi, E. S. Alnemri, A conserved XIAP-interaction motif in caspase-9 and Smac/DIABLO regulates caspase activity and apoptosis. *Nature* **410**, 112–116 (2001).

33. M. C. Sweeney, X. Wang, J. Park, Y. Liu, D. Pei, Determination of the sequence specificity of XIAP BIR domains by screening a combinatorial peptide library. *Biochemistry* **45**, 14740–14748 (2006).

34. Z. Liu, C. Sun, E. T. Olejniczak, R. P. Meadows, S. F. Betz, T. Oost, J. Herrmann, J. C. Wu, S. W. Fesik, Structural basis for binding of Smac/DIABLO to the XIAP BIR3 domain. *Nature* **408**, 1004–1008 (2000).

35. G. Wu, J. Chai, T. L. Suber, J.-W. Wu, C. Du, X. Wang, Y. Shi, Structural basis of IAP recognition by Smac/DIABLO. *Nature* **408**, 1008–1012 (2000).

36. J. Chai, C. du, J.-W. Wu, S. Kyin, X. Wang, Y. Shi, Structural and biochemical basis of apoptotic activation by Smac/DIABLO. *Nature* **406**, 855–862 (2000).

37. W. Neupert, J. M. Herrmann, Translocation of proteins into mitochondria. *Annu. Rev. Biochem.* **76**, 723–749 (2007).

38. M. C. Franklin, S. Kadkhodayan, H. Ackerly, D. Alexandru, M. D. Distefano, L. O. Elliott, J. A. Flygare, G. Mausisa, D. C. Okawa, D. Ong, D. Vucic, K. Deshayes, W. J. Fairbrother, Structure and function analysis of peptide antagonists of melanoma inhibitor of apoptosis (ML-IAP). *Biochemistry* **42**, 8223–8231 (2003).

39. T. K. Oost, C. Sun, R. C. Armstrong, A.-S. Al-Assaad, S. F. Betz, T. L. Deckwerth, H. Ding, S. W. Elmore, R. P. Meadows, E. T. Olejniczak, A. Oleksijew, T. Oltersdorf, S. H. Rosenberg, A. R. Shoemaker, K. J. Tomaselli, H. Zou, S. W. Fesik, Discovery of potent antagonists of the antiapoptotic protein XIAP for the treatment of cancer. *J. Med. Chem.* **47**, 4417–4426 (2004).

40. R. A. Kipp, M. A. Case, A. D. Wist, C. M. Cresson, M. Carrell, E. Griner, A. Wiita, P. A. Albiniak, J. Chai, Y. Shi, M. F. Semmelhack, G. L. McLendon, Molecular targeting of inhibitor of apoptosis proteins based on small molecule mimics of natural binding partners. *Biochemistry* **41**, 7344–7349 (2002).

41. S. Deng, R. Marmorstein, Protein N-terminal acetylation: Structural basis, mechanism, versatility, and regulation. *Trends Biochem. Sci.*, S0968-0004(20)30202-4 (2020).

42. F. Frottin, A. Martinez, P. Peynot, S. Mitra, R. C. Holz, C. Giglione, T. Meinnel, The proteomics of N-terminal methionine cleavage. *Mol. Cell. Proteomics* **5**, 2336–2349 (2006).

43. O.-K. Song, X. Wang, J. H. Waterborg, R. Sternglanz, An N^{α}-acetyltransferase responsible for acetylation of the N-terminal residues of histones H4 and H2A. *J. Biol. Chem.* **278**, 38109–38112 (2003).

44. K. Hole, P. van Damme, M. Dalva, H. Aksnes, N. Glomnes, J. E. Varhaug, J. R. Lillehaug, K. Gevaert, T. Arnesen, The human *N*-alpha-acetyltransferase 40 (hNaa40p/hNatD) is conserved from yeast and N-terminally acetylates histones H2A and H4. *PLOS ONE* **6**, e24713 (2011).

45. P. Van Damme, R. Evjenth, H. Foyn, K. Demeyer, P.-J. De Bock, J. R. Lillehaug, J. Vandekerckhove, T. Arnesen, K. Gevaert, Proteome-derived peptide libraries allow detailed analysis

of the substrate specificities of N^{α}-acetyltransferases and point to hNaa10p as the post-translational actin N^{α}-acetyltransferase. *Mol. Cell. Proteomics* **10**, M110.004580 (2011).

46. A. Drazic, H. Aksnes, M. Marie, M. Boczkowska, S. Varland, E. Timmerman, H. Foyn, N. Glomnes, G. Rebowski, F. Impens, K. Gevaert, R. Dominguez, T. Arnesen, NAA80 is actin's N-terminal acetyltransferase and regulates cytoskeleton assembly and cell motility. *Proc. Natl. Acad. Sci. U.S.A.* **115**, 4399–4404 (2018).

47. M. Goris, R. S. Magin, H. Foyn, L. M. Myklebust, S. Varland, R. Ree, A. Drazic, P. Bhambra, S. I. Støve, M. Baumann, B. E. Haug, R. Marmorstein, T. Arnesen, Structural determinants and cellular environment define processed actin as the sole substrate of the N-terminal acetyltransferase NAA80. *Proc. Natl. Acad. Sci. U.S.A.* **115**, 4405–4410 (2018).

48. B. P. Eckelman, G. S. Salvesen, The human anti-apoptotic proteins cIAP1 and cIAP2 bind but do not inhibit caspases. *J. Biol. Chem.* **281**, 3254–3260 (2006).

49. F. L. Scott, J.-B. Denault, S. J. Riedl, H. Shin, M. Renatus, G. S. Salvesen, XIAP inhibits caspase-3 and -7 using two binding sites: Evolutionarily conserved mechanism of IAPs. *EMBO J.* **24**, 645–655 (2005).

50. E. N. Shiozaki, J. Chai, D. J. Rigotti, S. J. Riedl, P. Li, S. M. Srinivasula, E. S. Alnemri, R. Fairman, Y. Shi, Mechanism of XIAP-mediated inhibition of caspase-9. *Mol. Cell* **11**, 519–527 (2003).

51. S. Fulda, D. Vucic, Targeting IAP proteins for therapeutic intervention in cancer. *Nat. Rev. Drug Discov.* **11**, 109–124 (2012).

52. S. Fulda, Smac mimetics to therapeutically target IAP proteins in cancer. *Int. Rev. Cell Mol. Biol.* **330**, 157–169 (2017).

53. S. T. Beug, C. E. Beauregard, C. Healy, T. Sanda, M. St-Jean, J. Chabot, D. E. Walker, A. Mohan, N. Earl, X. Lun, D. L. Senger, S. M. Robbins, P. Staeheli, P. A. Forsyth, T. Alain, E. C. La Casse, R. G. Korneluk, Smac mimetics synergize with immune checkpoint inhibitors to promote tumour immunity against glioblastoma. *Nat. Commun.* **8**, 14278 (2017).

54. Z. Wang, Z. Wang, J. Guo, Y. Li, J. H. Bavarva, C. Qian, M. C. Brahimi-Horn, D. Tan, W. Liu, Inactivation of androgen-induced regulator ARD1 inhibits androgen receptor acetylation and prostate tumorigenesis. *Proc. Natl. Acad. Sci. U.S.A.* **109**, 3053–3058 (2012).

55. C.-F. Lee, D. S.-C. Ou, S.-B. Lee, L.-H. Chang, R.-K. Lin, Y.-S. Li, A. K. Upadhyay, X. Cheng, Y.-C. Wang, H.-S. Hsu, M. Hsiao, C.-W. Wu, L.-J. Juan, hNaa10p contributes to tumorigenesis by facilitating DNMT1-mediated tumor suppressor gene silencing. *J. Clin. Invest.* **120**, 2920–2930 (2010).

56. H. Xu, B. Jiang, L. Meng, T. Ren, Y. Zeng, J. Wu, L. Qu, C. Shou, *N*-α-acetyltransferase 10 protein inhibits apoptosis through RelA/p65-regulated MCL1 expression. *Carcinogenesis* **33**, 1193–1202 (2012).

57. T. Arnesen, D. Gromyko, F. Pendino, A. Ryningen, J. E. Varhaug, J. R. Lillehaug, Induction of apoptosis in human cells by RNAi-mediated knockdown of hARD1 and NATH, components of the protein *N*-α-acetyltransferase complex. *Oncogene* **25**, 4350–4360 (2006).

58. C. H. Yi, D. K. Sogah, M. Boyce, A. Degterev, D. E. Christofferson, J. Yuan, A genome-wide RNAi screen reveals multiple regulators of caspase activation. *J. Cell Biol.* **179**, 619–626 (2007).

59. H.-K. Kim, R.-R. Kim, J.-H. Oh, H. Cho, A. Varshavsky, C.-S. Hwang, The N-terminal methionine of cellular proteins as a degradation signal. *Cell* **156**, 158–169 (2014).

60. F. Pietrocola, L. Galluzzi, J. M. Bravo-San Pedro, F. Madeo, G. Kroemer, Acetyl coenzyme A: A central metabolite and second messenger. *Cell Metab.* **21**, 805–821 (2015).

61. R. T. Timms, Z. Zhang, D. Y. Rhee, J. W. Harper, I. Koren, S. J. Elledge, A glycine-specific N-degron pathway mediates the quality control of protein *N*-myristoylation. *Science* **365**, eaaw4912 (2019).

62. S.-E. Ong, B. Blagoev, I. Kratchmarova, D. B. Kristensen, H. Steen, A. Pandey, M. Mann, Stable isotope labeling by amino acids in cell culture, SILAC, as a simple and accurate approach to expression proteomics. *Mol. Cell. Proteomics* **1**, 376–386 (2002).

63. S.-E. Ong, M. Mann, Mass spectrometry–based proteomics turns quantitative. *Nat. Chem. Biol.* **1**, 252–262 (2005).

64. E. Mastrangelo, F. Cossu, M. Milani, G. Sorrentino, D. Lecis, D. Delia, L. Manzoni, C. Drago, P. Seneci, C. Scolastico, V. Rizzo, M. Bolognesi, Targeting the X-linked inhibitor of apoptosis protein through 4-substituted azabicyclo[5.3.0]alkane smac mimetics. Structure, activity, and recognition principles. *J. Mol. Biol.* **384**, 673–689 (2008).

65. O. Kleifeld, A. Doucet, A. Prudova, U. auf dem Keller, M. Gioia, J. N. Kizhakkedathu, C. M. Overall, Identifying and quantifying proteolytic events and the natural N terminome by terminal amine isotopic labeling of substrates. *Nat. Protoc.* **6**, 1578–1611 (2011).

66. B. Metz, G. F. A. Kersten, P. Hoogerhout, H. F. Brugghe, H. A. M. Timmermans, A. de Jong, H. Meiring, J. . Hove, W. E. Hennink, D. J. A. Crommelin, W. Jiskoot, Identification of formaldehyde-induced modifications in proteins: Reactions with model peptides. *J. Biol. Chem.* **279**, 6235–6243 (2004).

67. X. Zhang, J. Ye, P. Hojrup, A proteomics approach to study *in vivo* protein N^{α}-modifications. *J. Proteomics* **73**, 240–251 (2009).

68. N. C. Hubner, A. W. Bird, J. Cox, B. Splettstoesser, P. Bandilla, I. Poser, A. Hyman, M. Mann, Quantitative proteomics combined with BAC TransgeneOmics reveals in vivo protein interactions. *J. Cell Biol.* **189**, 739–754 (2010).

69. J. Cox, M. Mann, MaxQuant enables high peptide identification rates, individualized p.p.b.-range mass accuracies and proteome-wide protein quantification. *Nat. Biotechnol.* **26**, 1367–1372 (2008).

70. J. Cox, M. Y. Hein, C. A. Luber, I. Paron, N. Nagaraj, M. Mann, Accurate proteome-wide label-free quantification by delayed normalization and maximal peptide ratio extraction, termed MaxLFQ. *Mol. Cell. Proteomics* **13**, 2513–2526 (2014).

71. S. Tyanova, T. Temu, P. Sinitcyn, A. Carlson, M. Y. Hein, T. Geiger, M. Mann, J. Cox, The Perseus computational platform for comprehensive analysis of (prote)omics data. *Nat. Methods* **13**, 731–740 (2016).

72. C. A. Schneider, W. S. Rasband, K. W. Eliceiri, NIH Image to ImageJ: 25 years of image analysis. *Nat. Methods* **9**, 671–675 (2012).

73. H.-C. Yen, Q. Xu, D. M. Chou, Z. Zhao, S. J. Elledge, Global protein stability profiling in mammalian cells. *Science* **322**, 918–923 (2008).

74. A. Bachmair, D. Finley, A. Varshavsky, In vivo half-life of a protein is a function of its amino-terminal residue. *Science* **234**, 179–186 (1986).